BJ www.biochemj.org

Biochem. J. (2012) **442**, 381–389 (Printed in Great Britain) doi:10.1042/BJ20111363

Membrane integration of a mitochondrial signal-anchored protein does not require additional proteinaceous factors

Elisa MERKLINGER*, Yana GOFMAN†, Alexej KEDROV‡, Arnold J. M. DRIESSEN‡, Nir BEN-TAL§, Yechiel SHAI¶ and Doron RAPAPORT*[1]

*Interfaculty Institute of Biochemistry, Hoppe-Seyler-Strasse 4, University of Tübingen, 72076 Tübingen, Germany, †Helmholtz-Zentrum, Max-Planck-Strasse 1, 21502 Geesthacht, Germany, ‡Department of Molecular Microbiology, Groningen Biomolecular Sciences and Biotechnology Institute and the Zernike Institute for Advanced Materials, University of Groningen, 9747 AG Groningen, The Netherlands, §Department of Biochemistry and Molecular Biology, The George S. Wise Faculty of Life Sciences, Tel Aviv University, Tel Aviv 69978, Israel, and ¶Department of Biological Chemistry, The Weizmann Institute of Science, Rehovot 76100, Israel

The MOM (mitochondrial outer membrane) contains SA (signal-anchored) proteins that bear at their N-terminus a single hydrophobic segment that serves as both a mitochondrial targeting signal and an anchor at the membrane. These proteins, like the vast majority of mitochondrial proteins, are encoded in the nucleus and have to be imported into the organelle. Currently, the mechanisms by which they are targeted to and inserted into the OM (outer membrane) are unclear. To shed light on these issues, we employed a recombinant version of the SA protein OM45 and a synthetic peptide corresponding to its signal-anchor segment. Both forms are associated with isolated mitochondria independently of cytosolic factors. Interaction with mitochondria was diminished when a mutated form of the signal-anchor was employed. We demonstrate that the signal-anchor peptide acquires an α-helical structure in a lipid environment and adopted a TM (transmembrane) topology within artificial lipid bilayers. Moreover, the peptide's affinity to artificial membranes with OM-like lipid composition was much higher than that of membranes with ER (endoplasmic reticulum)-like lipid composition. Collectively, our results suggest that SA proteins are specifically inserted into the MOM by a process that is not dependent on additional proteins, but is rather facilitated by the distinct lipid composition of this membrane.

Key words: ergosterol, mitochondrion, outer membrane, signal-anchored protein (SA protein).

INTRODUCTION

Proteins residing in the MOM (mitochondrial outer membrane) facilitate various interactions between the organelle and the rest of the eukaryotic cell. All of these proteins are encoded in the nucleus and synthesized on cytosolic ribosomes. In contrast with most mitochondrial proteins that contain N-terminal cleavable mitochondrial presequences, all MOM proteins carry internal non-cleavable targeting and sorting signals [1–3]. These signals assure their specific targeting to the organelle and insertion into the lipid bilayer.

MOM proteins can be divided into those that contain only one TM (transmembrane) domain and those that are embedded in the membrane with several α-helical segments or as β-barrel structure. The SA (signal-anchored) proteins, which belong to the first group, owe their name to a short portion of their N-terminus that serves as both a mitochondrial targeting signal and an anchor to the MOM [4]. The large remaining portion of the protein is exposed to the cytosol. Verified members of this family in fungi include the receptor components of the TOM (translocase of outer mitochondrial membrane) complex, Tom20 and Tom70, and two additional proteins: OM45 (outer membrane 45) and the OM isoform of Mcr1 (momMcr1). The targeting signal of these proteins consists of the TM segment and positively charged flanking regions [3,4].

A topologically related group are the tail-anchored OM proteins that have an α-helical TM domain in their C-terminus and a large N-terminally positioned domain, exposed to the cytosol [5]. The targeting signal in these proteins and their mechanism of membrane integration was studied in some detail [6–9]. However, whereas the targeting information in tail-anchored proteins resides in the C-terminus, meaning that they have to be inserted into the membrane by a post-translational mechanism, some recognition of the N-terminal signal-anchor segment can occur while the rest of the polypeptide chain is still being synthesized. Hence, the biogenesis process of SA proteins can be completely different from that of the tail-anchored proteins.

Several lines of evidence suggest that import of SA protein does not require any of the known import components. First, it was demonstrated that mitochondrial targeting of Tom20 and Tom70 is not affected by either blocking the import receptors by specific antibodies or removing them upon proteolytic treatment [10,11]. Similarly, membrane insertion of SA proteins appears to be independent of the import pore formed by the TOM complex [11–13]. Despite the aforementioned similarities, it appears as if SA proteins do not share a common mechanism of targeting and insertion. Whereas OM45 and momMcr1 follow a still uncharacterized membrane integration pathway, the Tom receptors seem to use another pathway. It was proposed that another OM protein, Mim1 promotes both insertion of Tom20 and Tom70 into the OM and their final assembly into the TOM core complex [14–16]. Considering the observations described above, we previously suggested that proteins such as OM45 and momMcr1 can be inserted into the OM in a process that does not

Abbreviations used: ATR-FTIR, attenuated total reflectance-Fourier transform IR; CL, cardiolipin; DCM, dichlormethan; DIEA, *N*,*N*-diisopropylethylamine; DMF, dimethylformamide; ER, endoplasmic reticulum; Fmoc, fluoren-9-ylmethoxycarbonyl; ITC, isothermal titration calorimetry; LPC, L-α-lysophosphatidylcholine; LUV, large unilamellar vesicle; MBHA, p-methylbenzhydrylamine; MC, Monte Carlo; MOM, mitochondrial outer membrane; NBD-F, 7-nitrobenz-2-oxa-1,3-diazole fluoride; OM, outer membrane; PC, phosphatidylcholine; PE, phosphatidylethanolamine; PI, phosphatidylinositol; PS, phosphatidylserine; SA, signal-anchored; TAMRA, 6-carboxytetramethylrhodamine; TFA, trifluoroacetic acid; TM, transmembrane; TOM, translocase of outer mitochondrial membrane.

[1] To whom correspondence should be addressed (email doron.rapaport@uni-tuebingen.de).

require the assistance of the known import components [13,17]. However, this model does not exclude the possibility that an as yet unknown OM protein is involved, and our detailed understanding of the mechanisms that govern the membrane integration of these proteins is still rather vague.

In order to shed light on the biogenesis of this special group of proteins, we used a recombinant OM45 protein and synthesized a peptide corresponding to the signal-anchor segment of the protein. Both forms, but not their mutated variants, were able to associate with isolated mitochondria. Our results indicate that the OM45 peptide can adopt an α-helical conformation in a lipid environment and can tightly bind to protein-free phospholipid bilayers. Importantly, the low ergosterol content of the MOM appears to play an important role in the biogenesis process. Taken together, our findings support a mechanism where SA proteins can be inserted into the MOM in a process that depends on the unique lipid composition of this membrane, but is independent of additional proteins.

EXPERIMENTAL

Materials

Rink amide-MBHA (p-methylbenzhydrylamine) resin and Fmoc (fluoren-9-ylmethoxycarbonyl) amino acids were obtained from Calbiochem-Novabiochem. Other reagents used for peptide synthesis included TFA (trifluoroacetic acid), piperidine, DIEA (*N*,*N*-diisopropylethylamine), NMM (*N*-methylmorpholine), HOBT (*N*-hydroxybenzotriazole hydrate), HBTU [2-(1*H*-benzotriazol-1-yl)-1,1,3,3-tetramethyluronium hexafluorophosphate], DCM (dichlormethan; peptide synthesis grade) and DMF (dimethylformamide; peptide synthesis grade) (all from Biolab). 4-Chloro-NBD-F (7-nitrobenz-2-oxa-1,3-diazole fluoride) was purchased from Sigma and TAMRA (6-carboxytetramethylrhodamine) succinimidyl ester was from Molecular Probes. Egg LPC (L-α-lysophosphatidylcholine) and PI (phosphatidylinositol) were purchased from Sigma, PC (phosphatidylcholine), PE (phosphatidylethanolamine), PS (phosphatidylserine) and CL (cardiolipin) (diphosphatidylglycerol) were from Avanti, and ergosterol was from Larodan.

Construction and purification of recombinant proteins

DNA sequences encoding either full-length OM45, its cytosolic domain (lacking residues 1–38) or a mutant version of the full-length protein (R4E, K26E) were cloned into the vector pET28a (Novagen), which includes a C-terminal His_6 tag. The constructs were transformed into *Escherichia coli* cells (Rosetta2 DE3) and grown at 37 °C to D_{600} of 0.6 before protein expression was induced with 0.5 mM isopropyl β-D-thiogalactoside. Cells were grown for an additional 4 h at 30 °C and harvested by centrifugation. Next, the cells were resuspended in lysis buffer (50 mM sodium phosphate, 300 mM sodium chloride and 10 mM imidazole, pH 8.0) and lysis was performed by shaking for 1 h at 4 °C in the presence of PMSF, lysozyme and RNase followed by sonification. The homogenate was centrifuged and the supernatant was loaded on to a column containing Ni-NTA (Ni^{2+}-nitrilotriacetate)-agarose beads (Qiagen) and washed with 20 ml of lysis buffer with 20 mM imidazole. Elution of the protein was accomplished with 300 mM imidazole in lysis buffer. Purity and homogeneity of the proteins were confirmed by SDS/PAGE.

Peptide synthesis, fluorescent labelling and purification

Peptides were synthesized by an Fmoc solid-phase method on Rink amide resin. Cleavage of the peptides from the MBHA resin resulted in the amidation of the C-terminus. To label the peptides, the Fmoc protecting group at the N-terminus of the resin-bound peptides was removed by incubation with piperidine. All of the other reactive amine groups of the attached peptides were kept protected under these conditions. The resin-bound peptides were washed twice with DMF, and then treated with either NBD-F or TAMRA in anhydrous DMF containing 2 % DIEA, leading to the formation of a resin-bound N-NBD or N-rhodamine peptide respectively. After 1 h (NBD) or 24 h (TAMRA), the resin was washed with DMF and then with methylene chloride. To label the ε-amino group of Lys^{26} with the NBD group, the following procedure was applied. The MTT [3-(4,5-dimethylthiazol-2-yl)-2,5-diphenyl-2*H*-tetrazolium bromide] side chain protecting group, was removed under mild acidic conditions (2 × 1 min of 5 % TFA in DCM and 30 min of 1 % TFA in DCM), enabling the conjugation of the fluorophore after capping of the N-terminus with 1 M acetic anhydride and 0.3 M triethylamine in anhydrous DMF.

All of the peptides were purified by RP-HPLC (reversed-phase-HPLC) on a C4 RP Bio-Rad semi-preparative column. The column was eluted with a 40 min linear gradient of acetonitrile in water, containing 0.05 % TFA, at a flow rate of 1.8 ml/min. The purified peptides were further subjected to electrospray MS to confirm their molecular mass.

Binding of recombinant proteins and synthetic peptides to isolated mitochondria

Isolated mitochondria (20 μg) were incubated in SEM buffer (250 mM sucrose, 1 mM EDTA and 10 mM Mops-KOH, pH 7.2) in the presence or absence of 100 mM KCl with 4 μg of recombinant purified OM45 proteins for 20 min at room temperature (21 °C) and subsequently layered over a 60 % (w/v) sucrose cushion. After centrifugation (40 000 ***g***, 40 min, 4 °C) the supernatant was removed and proteins were precipitated. The layer between the cushion and the supernatant (5 % of total volume) was diluted and centrifuged (20 000 ***g***, 15 min, 4 °C). All fractions were subjected to SDS/PAGE and Western blot analysis. For the mitochondria–peptide interaction, 1 μM fluorescently labelled peptide was used and 100 μl fractions were collected. All fractions were analysed for their fluorescence and were analysed by SDS/PAGE and immunodecoration.

Preparation of LUVs (large unilamellar vesicles)

Thin films of a mixture of PC, PE, PI, CL and PS (molar ratio of 46:35:13:4:2 respectively) for OM-like LUVs or of PC, PE, PI, PS (54:25:11:10 respectively) containing 0.18 mol of ergosterol/mol of phospholipids for ER (endoplasmic reticulum)-like LUVs were generated from a solution of the lipids in a 2:1 (v/v) mixture of chloroform/methanol that was dried during rotation. The films were freeze-dried overnight, sealed with $Ar_{(g)}$, and stored at − 20 °C. To form vesicles, the films were suspended in PBS and vortex-mixed for 1.5 min. The lipid suspension underwent five cycles of freezing–thawing and then vesicles were extruded through polycarbonate membranes with 1.0 and then 0.2 μm pore diameters. The shape and size of the formed LUVs were verified by negative-staining electron microscopy.

Fluorescence measurements

Changes in the fluorescence of NBD-labelled peptides were measured upon binding to vesicles. LUVs (100 μM final concentration) were added to 400 μl of PBS containing 1 μM NBD-labelled peptide. Fluorescence measurements were

performed at room temperature, with λ_{ex} set at 467 nm (10 nm slit) and λ_{em} scan at 500–600 nm (10 nm slits) or set constant at 530 nm. The extent of insertion was measured by adding increasing amounts of LUVs to a fixed amount of peptide (0.2–1 μM). After the signal reached a plateau, proteinase K (125 μg/ml final concentration) was added.

ITC (isothermal titration calorimetry)

ITC was performed using an ITC_{200} microcalorimeter (MicroCal; GE Healthcare). Small aliquots (3 μl) of the SA-peptide solution (20 μM) were injected into a solution of LUVs (2 mM) in a cell volume of $\sim$200 μl. Alternatively, small aliquots of an LUV solution (4 mM) were injected into a solution of peptide (10 μM). Control experiments included titration of peptide into buffer solution, injection of vesicle solution into buffer and the addition of buffer into LUV solution. The heat released upon dilution, determined in these control experiments was subtracted from the heat of the peptide–liposome binding reactions. Binding isotherms were integrated and analysed using Origin®7 software according to a 'one binding site' model.

Further methods are described in the Supplementary Online Data (available at http://www.BiochemJ.org/bj/442/bj4420381add.htm).

RESULTS

Recombinant OM45 and a signal-anchor peptide specifically bind isolated mitochondria

To study binding of SA proteins to the MOM in the absence of cytosolic chaperones, we used the MOM SA protein OM45 as a model protein. To follow binding, we analysed the sedimentation behaviour on a sucrose cushion of isolated organelle, recombinant His_6-tagged OM45 purified from *E. coli* cells, and a mixture containing both components. Three fractions were collected after centrifugation: (i) an upper fraction that contains soluble unbound proteins, (ii) a middle fraction, where mitochondria was enriched, collected from the interface between the sucrose cushion and the buffer and (iii) a lower fraction that contained the pellet. Free OM45 was mainly present at the top fraction of the gradient, whereas a subpopulation of free OM45 molecules was also detected in the lower pellet fraction (Figure 1A). We suggest that this latter population represents aggregated molecules. Incubation of the recombinant protein with isolated mitochondria in the presence of 100 mM salt prior to centrifugation resulted in co-migration of these components in the middle fraction. In contrast, a protein corresponding to the cytosolic domain of OM45 did not bind to the isolated organelle under these conditions (Figure 1A). Notably, the binding of full-length OM45 was not affected by trypsin-mediated removal of the exposed domains of protease-sensitive mitochondrial surface receptors (Figure 1A).

To verify the specificity of this binding assay, we used a recombinant variant of OM45 where Arg^4 and Lys^{26} within the signal-anchor segment were changed to Glu^4 and Glu^{26}, thus changing the net charge of the regions flanking the TM helix from $+5$ to $+1$. We previously observed that these mutations dramatically reduced the ability of the corresponding signal-anchor to mediate insertion of a model protein into the MOM [18]. In contrast with the native protein that was detected primarily in the bound fraction, a large portion of the mutated protein remained in the upper unbound fraction (Figure 1B). Hence, in accordance with our previous observation, the mutated protein demonstrates a reduced capacity to interact with isolated mitochondria. We next asked whether the mitochondria-associated OM45 is only attached on the surface of the organelle or also integrated into the membrane. To that end, the mitochondrial fraction was extracted after the binding reaction with alkaline solution and centrifuged. To allow comparison with the variants that lack the SA domain, the binding experiment was performed in a buffer lacking salt where small amounts of the cytosolic domain of OM45 can associate with the organelle (Figure 1C). Notably, whereas the cytosolic domain of OM45 is found solely in the soluble fraction, approximately a third of the full-length protein molecules are embedded in the membrane (Figure 1C). We conclude that binding

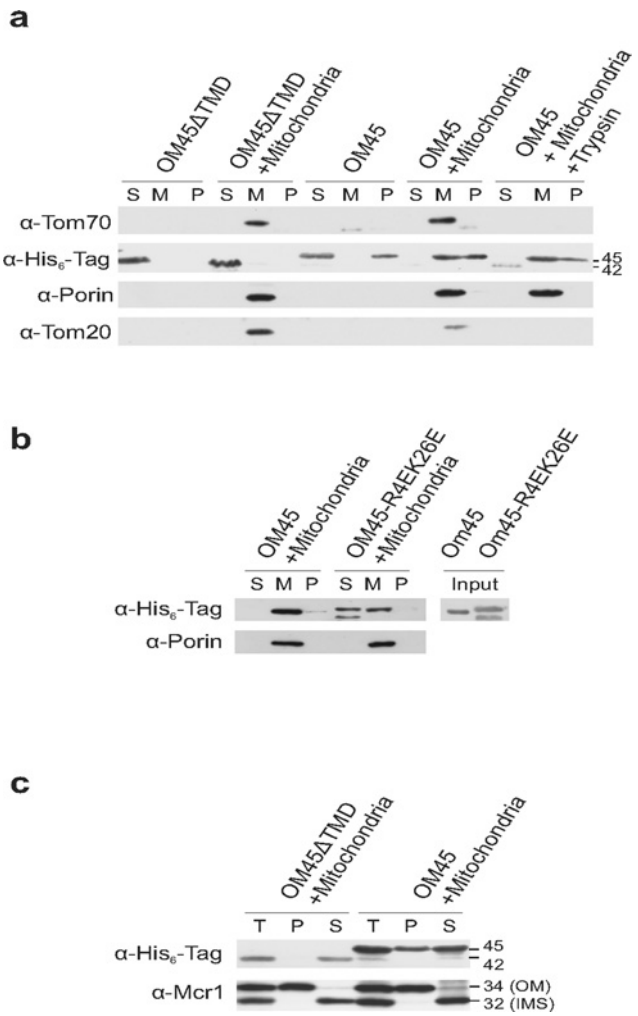

Figure 1 Binding of the OM45 protein to mitochondria

(**a**) Recombinant full-length OM45 protein (OM45) or its cytosolic domain (OM45△TMD) were loaded on a sucrose cushion either alone or after pre-incubation with mitochondria (20 μg) in a buffer containing 100 mM KCl. In one sample, mitochondria pretreated with trypsin was used. Three fractions were collected after centrifugation: supernatant (S), a middle fraction (M) containing the mitochondria and a lower fraction in the cushion (P). The samples were analysed by SDS/PAGE and immunodecorated with antibodies against the His_6-tag, Tom70 and Tom20 (exposed OM receptor proteins), and porin (membrane-embedded OM protein). (**b**) Recombinant full-length OM45 or its charge variant (OM45-R4EK26E) were treated as described in (**a**). Proteins before loading on to the sucrose cushion were analysed (right-hand panel). (**c**) Recombinant full-length OM45 protein or its cytosolic domain was incubated with mitochondria in a buffer lacking salt. The samples were treated as described in (**a**) and the middle fraction was collected and halved. One aliquot was left untreated (T), whereas the second aliquot was subjected first to alkaline extraction and then centrifuged to discriminate between membrane proteins in the pellet (P) and soluble proteins in the supernatant (S). The samples were subjected to SDS/PAGE and immunodecoration with antibodies against OM45 and Mcr1. The latter protein has two isoforms: a 34 kDa form embedded in the OM and a 32 kDa soluble form in the mitochondrial intermembrane space.

and integration of recombinant OM45 into the OM can occur in the absence of cytosolic chaperones, and the assembly into the membrane depends on the SA domain.

The aforementioned experiments demonstrate that the signal-anchor segment is necessary for mitochondrial binding. In addition, we have previously demonstrated that the first 32 amino acid residues of OM45 are sufficient to target *in vivo* a passenger protein to mitochondria [18]. To further investigate the mechanism by which the SA segment integrates into the organelle OM, we used a synthetic peptide corresponding to residues 2–32 of OM45 (OM45-SA). The peptide was selectively labelled at either its N-terminus or at Lys^{28} with the fluorophore NBD. This fluorophore can be utilized for binding studies since its fluorescence spectrum and intensity reflects the environment in which the NBD group is located. In addition a variant where the N-terminus is labelled with tetramethyl rhodamine was prepared. To serve as control peptides, we also synthesized and labelled a peptide harbouring the charge mutations (R4E and K26E) in the SA segment (Figure 2A). Purified peptides were shown to be homogeneous (>95 %) by analytical HPLC and MS (results not shown).

To address the question whether the signal-anchor segment is able by itself to bind to mitochondria, we mixed the rhodamine-labelled peptides with isolated mitochondria. Next, the organelle was re-isolated by sedimentation on a sucrose cushion and fractions were collected. Importantly, rhodamine fluorescence of the native peptide and mitochondrial proteins were enriched in the same fractions. In contrast, the fluorescence of the mutated peptide was not detected in the mitochondria-containing fractions (Figure 2B). Thus this assay demonstrates specific binding of the native SA peptide to the organelle. To monitor whether the peptide is indeed integrated into the membrane, we incubated the isolated organelle with NBD-labelled peptide and then followed the emission spectrum of the NBD moiety. The addition of mitochondria to an aqueous solution of the peptide resulted in a dramatic increase in the fluorescence intensity of the NBD moiety and in the so-called 'blue-shift', a shift of the maximal emission to shorter wavelengths (Figure 2C). Of note these changes that demonstrate a shift of the NBD group to a more hydrophobic environment apparently upon integration into the OM were observed to a highly reduced extent with the mutant peptide (Figure 2C). To verify the insertion into the membrane, samples containing mitochondria-bound native peptide were treated with proteinase K. It is expected that a cleavage of an exposed N-terminus would result in the release of an NBD-containing fragment into the aqueous environment and subsequently a major reduction in the NBD fluorescence. Nevertheless, we observed that approximately 70 % of the fluorescence signal remained (Figure 2D). These results suggest that the majority of the peptide molecules were inserted into the membrane.

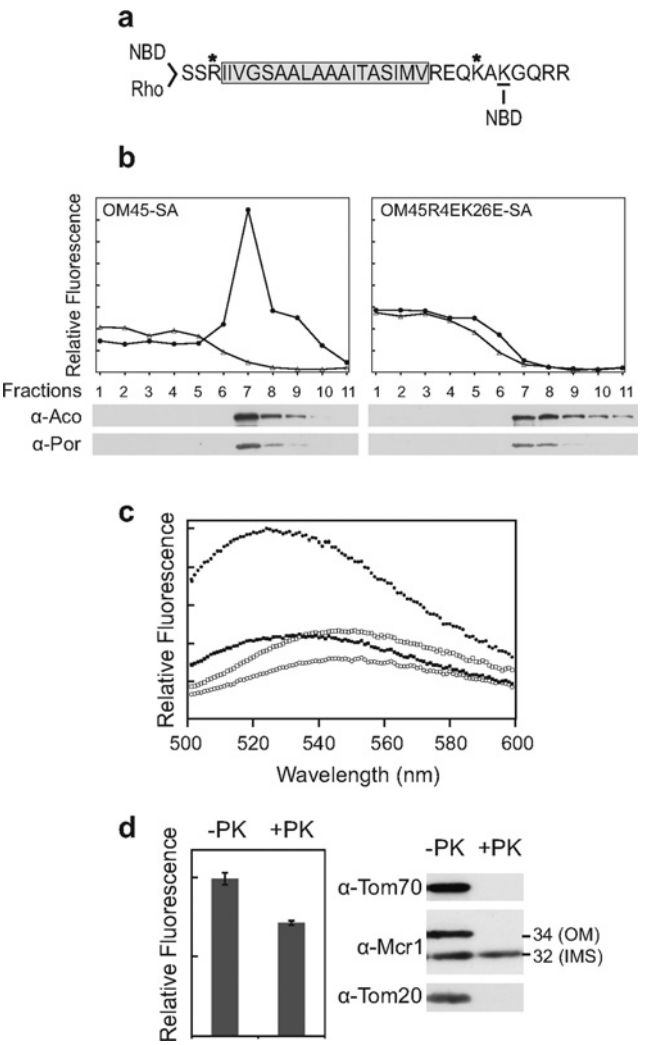

Figure 2 Signal-anchor peptide can bind to mitochondria

(**a**) Amino acid sequence of residues 2–32 of OM45. The putative TM helix of OM45 is within a box. The positions of the fluorescent probes are shown and the residues mutated in the R4E and K26E mutations are indicated by asterisks. Rho, rhodamine. (**b**) Mitochondria were incubated with rhodamine-labelled peptides before their re-isolation by centrifugation on top of a sucrose cushion. Ten different fractions were collected, their fluorescence emission was measured at 580 nm, and the relative fluorescence intensity of each fraction is presented. Bottom panels: proteins from the same fractions were precipitated and then analysed by SDS/PAGE and immunodecoration with antibodies against the mitochondrial marker proteins aconitase (Aco) and porin (Por). (**c**) Fluorescence emission spectra of 1 μM N-NBD-labelled native peptide and R4EK26E variant in buffer (open circles or open squares respectively) or in the presence of isolated mitochondria (closed circles or closed squares respectively). (**d**) Mitochondria were incubated with N-NBD native peptide. The samples were divided into two halves and one of them was incubated further on ice with proteinase K (PK) before the fluorescence emission was monitored (left-hand panel). Right-hand panel: proteins from both aliquots were analysed by SDS/PAGE and immunodecoration with antibodies against Tom20 and Tom70 (OM-exposed proteins), and against Mcr1.

Secondary structure of the OM45-SA peptide and its orientation within membranes

To better understand the structural requirements for membrane integration, we analysed by the CD method the secondary structure of the peptide in buffer or in the presence of LPC which provides a lipid-like environment, whereas in the former conditions the peptide acquired a mainly β-sheet conformation or was unstructured, the addition of the LPC resulted in conformations with mostly α-helical structure (Supplementary Figure S1 and Supplementary Table S1 available at http://www.BiochemJ.org/bj/442/bj4420381add.htm).

To further study the structure of the peptide in a lipid environment, we utilized ATR-FTIR (attenuated total reflectance-Fourier transform IR) spectroscopy. We first tested whether the addition of the peptide to the membrane affects the acyl-chain order of the phospholipid molecules. To that end, polarized ATR-FTIR was used to determine the orientation of the lipid membrane. The phospholipid composition (PC 46 %, PE 35 %, PI 13 %, CL 4 % and PS 2 %) was according to the published composition of the yeast MOM [19]. The symmetric [$\upsilon_{sym}(CH_2) \approx 2853\ cm^{-1}$] and the antisymmetric [$\upsilon_{antisym}(CH_2) \approx 2922\ cm^{-1}$] vibrations of lipid C – H bonds are perpendicular to the molecular axis of a fully extended hydrocarbon chain. The position of these

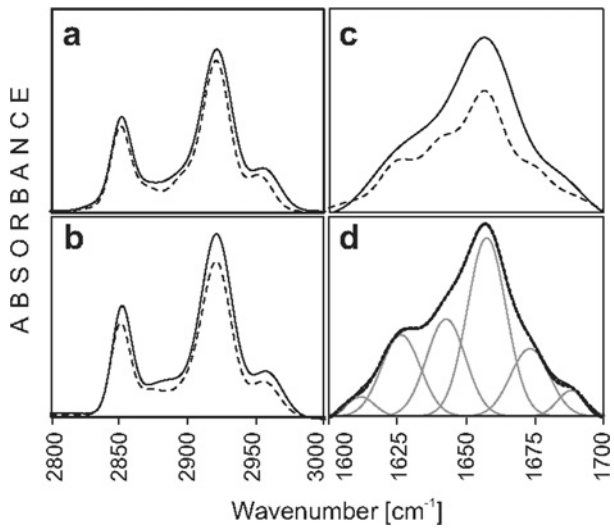

Figure 3 FTIR measurements of OM45-SA peptide in membrane environment

(**a** and **b**) ATR dichroism spectra of parallel (continuous lines) and perpendicular (dotted lines) polarized ATR-FTIR absorbance for the lipid CH_2 symmetric and anti-symmetric vibrations of PE/PI/PC/PS/CL multibilayers. (**a**) Lipids alone and (**b**) lipids in the presence of OM45-SA peptide. The peptide/lipid molar ratio was fixed at 1:50. (**c**) FTIR spectra of parallel (continuous line) and perpendicular (dotted line) polarized ATR-FTIR absorbance of amide I band of the OM45-SA peptide in the presence of PE/PI/PC/PS/CL multibilayers. All measurements were taken at a peptide/lipid molar ratio of 1:50. (**d**) The spectra in (**c**) were analysed using the curve fitting of the amide I band area assuming Gaussian line shape. The resulting deconvolution peaks are displayed under the fitting (black line).

peaks indicated that the membranes are predominantly in a native-like liquid-crystalline phase [20]. Measurement of the dichroism of IR light absorbance can reveal the order and orientation of the membrane sample relative to the prism surface [21]. The R value based on the stronger $\upsilon_{antisym}(CH_2)$ was 1.18 and the corresponding orientation order parameter, f, was calculated (based on $\upsilon_{antisym}$) to be 0.62. The effect of OM45-SA peptide on the multibilayer acyl-chains order can be estimated by comparing the CH_2-stretching dichroic ratio of peptide-free multibilayers with that obtained with membranes containing incorporated peptide. The results indicate that integration of the SA peptide into the membranes changed somewhat the lipid order (Figures 3A and 3B). The R values and the corresponding order parameter f, at peptide/lipid molar ratios of 1:50 was 1.12 and 0.59 respectively. Hence the peptide decreased the lipid order, reflecting a reorganization of the lipid molecules probably due to the presence of oblique-inserted peptide molecules.

To determine directly the orientation of the peptides within lipid bilayers, polarized ATR-FTIR was used. Spectra of the amide I region of the peptide bound to the multibilayers and their deconvoluted components are shown in Figures 3(C) and 3(D). According to this analysis 52 % of the peptide molecules are in an α-helical structure. This value is in a good agreement with the 58 % α-helical structure that was estimated according to the CD measurements (Supplementary Table S1). The R value was 1.63 and the order parameter, f (-0.18) was slightly negative, typical of helices oriented oblique to the membrane surface [22]. According to these parameters, an 'average' angle of 62° between the main axis of the peptide and the bilayer normal was obtained. We propose that this value actually results from a situation where approximately half of the molecules are in a surface conformation and the other half acquired the TM configuration. Such an average angle is also similar to that of peptides known to acquire a TM conformation [23]. Taken together, these structural studies suggest that the peptide can adopt an α-helical TM conformation in the presence of artificial lipid membranes.

Binding of the OM45-SA peptide to pure lipid vesicles

We next addressed the question whether a proteinaceous element has to be postulated in the insertion of SA proteins. To that end, the interaction of the OM45 peptides with protein-free lipid vesicles was analysed. LUVs were prepared from phospholipids in a composition similar to that of the MOM in yeast [19]. Addition of these LUVs to the NBD-labelled native or mutant peptide resulted in an enhancement in the fluorescence of the NBD group only in the case of the former peptide (Figures 4A and 4D). Hence addition of vesicles to the native peptide resulted in membrane integration of the NBD moiety. Interestingly, although the NBD group at the C-terminus of the native peptide displayed an enhancement of the fluorescence intensity in methanol, it failed to do so upon addition of LUVs (Figure 4B). The absence of such an increase probably indicates that the NBD group and the hydrophobic core of the membrane are distant from each other. While at the N-terminus only three residues separate the NBD group from the last amino acid of the putative TM segment, in the C-terminus this distance corresponds to six amino acids. Of note, we cannot exclude the unfavourable possibility that the NBD group at the C-terminus interferes with peptide binding to the membrane.

We then tested whether the peptide is indeed integrated into the lipid bilayer. The addition of proteinase K to the samples with the bound peptide resulted in an approximately 50 % reduction in the fluorescence intensity (Figure 4C). Hence it appears that approximately half of the peptide molecules are in the TM configuration. We excluded the possibility of peptide aggregation since no self-quenching of the rhodamine-labelled peptide was observed under these conditions ([24] and results not shown).

Is the unique lipid composition of the MOM important for the membrane integration of the OM45 peptide? The N-terminally NBD-labelled peptide was titrated with LUVs and the increase in the fluorescence intensity was monitored. Plotting this enhancement as a function of the vesicle concentration allowed us to determine the affinity of the peptide to the vesicles. This affinity was calculated to be $223 \pm 12\ \mu$M when LUVs lacking ergosterol and having the phospholipid composition of the MOM were used (Figure 4E). The binding of the peptide to CL-free vesicles was comparable with CL-containing LUVs, and the binding of the peptide to mitochondria lacking CL (isolated from the *cdr1*△ strain) was very similar to its binding to WT (wild-type) organelle (results not shown). Thus CL does not appear to play an important role in binding and integration of the OM45 peptide. We previously observed that elevated ergosterol levels interfere with the insertion of tail-anchored protein into lipid vesicles [9]. To check whether a similar effect can be observed with the signal-anchor peptide, we included 2, 10 or 20 % ergosterol in the mixture of the lipid vesicles. Adding these ergosterol-containing vesicles to the NBD-labelled peptide resulted in a strongly reduced enhancement in the fluorescence signal as compared with addition of ergosterol-free LUVs (Figures 4E and 4F).

To further investigate, in a quantitative manner, the role of the lipid composition in the membrane integration process, we studied its thermodynamics using ITC. To this end, a solution containing lipid vesicles with the composition of either the MOM or ER membrane was titrated into an ITC cell containing the

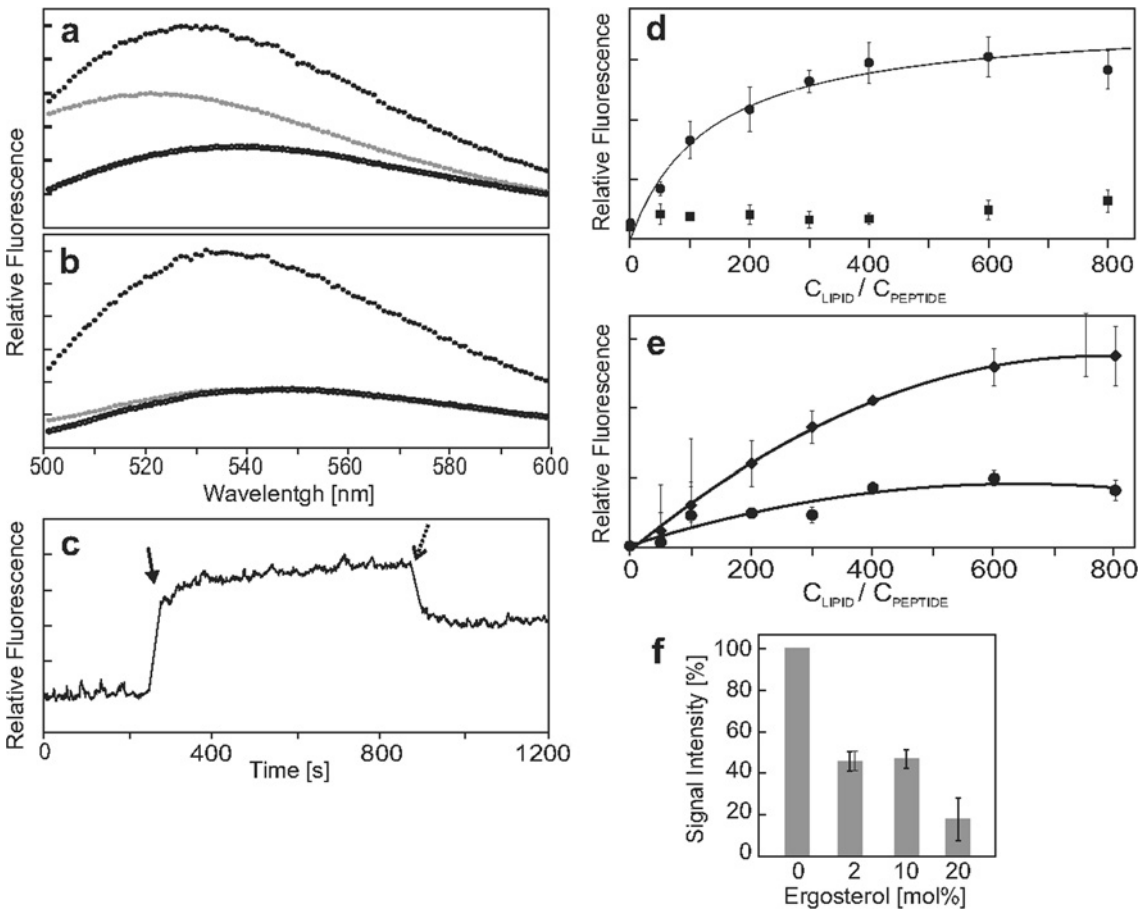

Figure 4 NBD-labelled OM45-SA peptide can integrate into artificial membrane vesicles

(**A**) Fluorescence emission spectra of 1 μM N-NBD-labelled native peptide in buffer (open circles), methanol (black closed circles) or in the presence of 100 μM PE/PI/PC/PS/CL LUV (grey closed circles). (**B**) The C-terminally labelled native peptide was analysed as in (**A**). (**C**) Representative experiment of proteolytic digestion of membrane-bound NBD labelled native peptide. The fluorescence emission of NBD-labelled peptide (1 μM) was monitored at 530 nm. The filled arrow indicates addition of 100 μM LUV and the dotted arrow the addition of 125 μg/ml proteinase K. (**D**) N-terminally NBD-labelled native peptide (circles) and its charge variant (squares) were incubated with increasing amounts of PE/PI/PC/PS/CL LUV. The fluorescence emission was monitored at 530 nm. (**E**) N-terminally NBD-labelled native peptide (0.5 μM) was incubated with increasing amounts of ergosterol-free PE/PI/PC/PS/CL LUV (diamonds) or with LUV supplemented with 10 % ergosterol (circles). The fluorescence emission was monitored at 530 nm. (**F**) NBD-labelled native peptide (0.5 μM) was incubated with increasing amounts of LUV lacking ergosterol or supplemented with 2, 10 or 20 % ergosterol. The fluorescence emission at 530 nm was monitored after each addition and that with the ergosterol-free LUV was set as 100 %. The presented values represent an average of all the employed lipid concentrations.

native OM45 peptide, and the heat amount released upon the peptide–lipid binding reaction was recorded (Figures 5A and 5B). Progressive vesicle injections produced decreasing exothermic heats as the availability of the peptide in the cell was gradually exhausted by association with the liposomes. We observed an elevated heat release upon binding of the SA-peptide to the vesicles with the MOM-like lipid composition. Analysis of the data resulted in enthalpy ($\triangle H$) of -31 kcal/mol (1 kcal = 4.184 kJ) for these membranes, whereas the binding to the ER-like vesicles was too weak to allow any fitting (Figures 5C and 5D). These results indicate that the peptide interaction with MOM-like membranes is thermodynamically favoured as compared with its interaction with ER-like membrane.

Next, we turned to investigate the kinetics of membrane binding of the SA peptide by utilizing a stopped-flow setup. The addition of the vesicles to the NBD-labelled peptide resulted in a biphasic increase in the fluorescence intensity. We observed a first phase where the fluorescence increased very fast (within <1 s) to approximately 90 % of the final intensity and a second slower phase that lasted several minutes (Figure 6A). Indeed, the first association rate constant was over 100-fold larger than the second one (Figure 6B). Similar biphasic behaviour was observed also for the membrane-active peptide mastoparan X [25]. Both the initial kinetics and the final fluorescence level were dependent on the amounts of the added vesicles. According to this dependency and considering only k_{obs1} we could calculate the K_d to be 244 μM, which is in an excellent agreement with the value obtained in the previous experiments (223 μM). In agreement with the aforementioned results, addition of vesicles containing 10 % ergosterol resulted in slower kinetics and a reduction in the fluorescence increase (results not shown).

A TM configuration of OM45-SA is thermodynamically more stable than a surface configuration

The results of the ATR-FTIR spectroscopy and the protection of the NBD probe from externally added protease suggest a TM configuration of the peptide. We asked whether this topology is indeed thermodynamically favoured. To that goal we used MC (Monte Carlo) simulations to calculate the free energy of the peptide in two configurations: parallel to the membrane surface

Table 1 Free energy values and energy decomposition for OM45 peptides in TM or surface configurations

Free energy values are shown in kcal/mol as means ± S.D. $\triangle G_{total}$ is the total free energy of membrane-association of the peptide (in each configuration). $\triangle G_{conf}$ is the free energy change due to membrane-induced conformational changes in the peptide. $\triangle G_{SIL}$ accounts mostly for the desolvation component of the process, including the favorable contribution of the hydrophobic effect. $\triangle G_{coul}$ stands for the Coulombic interactions between charged residues of the peptide and the (negative) surface charge of the membrane. $\triangle G_{def}$ is the free energy penalty associated with fluctuations of the membrane width around its resting (average) value.

Peptide/configuration	$\triangle G_{total}$	$\triangle G_{conf}$	$\triangle G_{SIL}$	$\triangle G_{coul}$	$\triangle G_{def}$
OM45/TM	− 11.9 ± 0.3	− 0.5 ± 0.2	− 6.6 ± 0.1	− 5.1 ± 0.0	0.2 ± 0.0
OM45/surface	− 8.7 ± 0.3	− 1.8 ± 0.1	− 2.4 ± 0.2	− 4.7 ± 0.2	0.2 ± 0.0
R4E,K26E/TM	− 6.1 ± 0.2	0.5 ± 0.3	− 6.5 ± 0.2	− 0.4 ± 0.1	0.3 ± 0.0
R4E,K26E/surface	− 1.3 ± 0.2	− 0.3 ± 0.2	0.0 ± 0.1	− 1.1 ± 0.1	0.2 ± 0.0

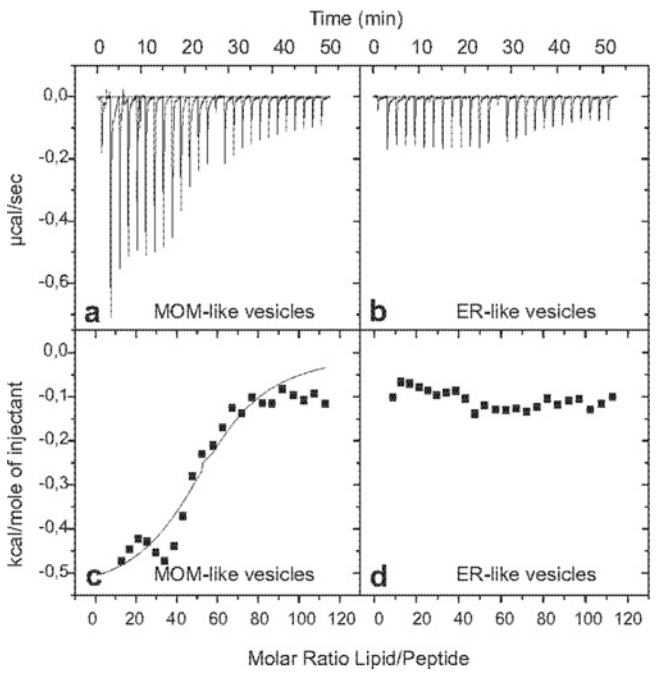

Figure 5 Binding of the SA-peptide to MOM-like and ER-like vesicles

(**a**) ITC experimental data on MOM LUVs titrated into the SA-peptide solution. (**b**) ITC experimental data of ER LUV injections. (**c** and **d**) Binding enthalpy calculated as an integral of the heat flow peaks and plotted as a function of lipid/peptide ratio for MOM-like LUVs (**c**) and ER-like LUVs (**d**).

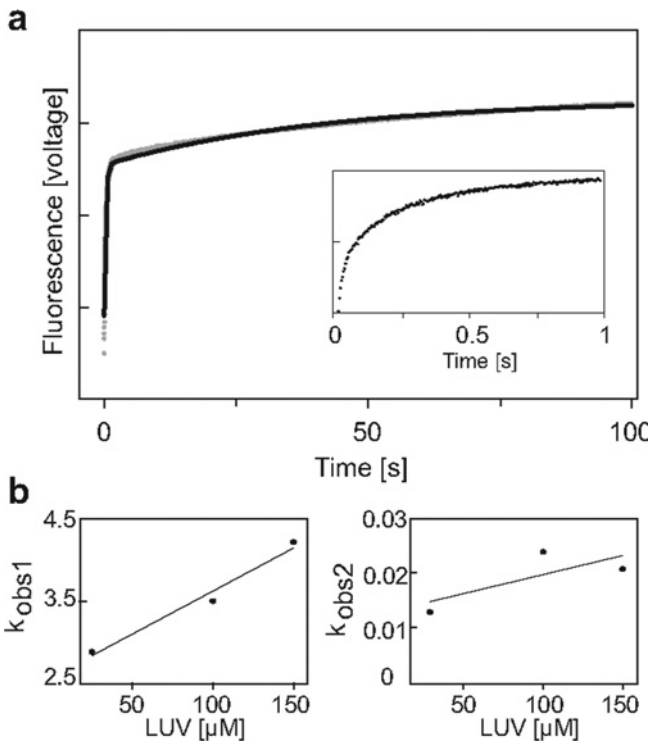

Figure 6 Kinetics of peptide binding to LUVs monitored using a stopped-flow setup

(**a**) Reaction of 1 μM NBD-labelled OM45-SA peptide with 100 μM LUVs under pseudo-first-order conditions. The fluorescence emission of N-NBD peptide was monitored at 530 nm with the excitation set at 467 nm. The inset displays an expansion of the signal in the first second. The solid line is the fit of the experimental data with a double exponential equation. (**b**) NBD-labelled OM45-SA peptide was incubated with increasing amounts of LUVs and the fluorescence signal was measured as described above. The dependence of the rate constants for the first (k_{obs1}) and second (k_{obs2}) components of the double-exponential reaction on the liposome concentration is presented in the left-hand and right-hand panel respectively.

and in TM orientation. For comparison, similar simulations were performed for the charge variant (R4E, K26E) peptide. The results show that the surface orientation of the native peptide is rather stable (Table 1), explaining the efficient and fast initial binding to lipid membranes (Figure 6). Interestingly, the values of the free energy decomposition obtained by the MC simulations suggest that the surface conformation of the peptide is stabilized by both solvation and electrostatic attractions (Table 1). However, the TM configuration is by far more stable, and therefore a reorganization of the peptide to the TM conformation would be favoured. This transformation is driven mostly by solvation since the electrostatic component is approximately the same in both configurations (Table 1). As the peptide has to cross the lipid core of the membrane, this re-orientation is expected to be slower than the initial binding; however, once occurred it will essentially not be reversible. In sharp contrast, the mutant peptide has less favourable electrostatic interactions with the lipid molecules and low stability in both the surface and TM orientations (Table 1). Taken together, these results in combination with the stopped-flow data can support a mechanism where the signal-anchor segment first binds at the surface of the organelle and then gets inserted into the membrane and acquires a TM conformation.

DISCUSSION

In the present study, we investigated the mechanism by which SA proteins are delivered from the cytosol into their final location at the MOM and subsequently inserted into this membrane. We

choose OM45 as a model protein since, in contrast with Tom20 and Tom70, it is not a subunit of the TOM complex. Subunits of this complex might represent a special case and indeed, the correct topology and assembly of the latter two proteins depends on pre-existing TOM complex [11,12]. Our results suggest that cytosolic factors are not required for the membrane integration of OM45. Interestingly, similar independency of cytosolic chaperones was suggested for some ER and mitochondrial tail-anchored proteins [7,26]. Of note, although *in vivo* such cytosolic chaperones might bind newly synthesized SA proteins, the results of the present study suggest that they are not strictly required for specific targeting and integration into the OM.

Our working hypothesis suggests that the SA domain interacts with the membrane according to a two-state model that was suggested for many membrane-active peptides [27–30]. According to this model, the peptide first binds rather fast to the lipid–water interface and forms α-helical structure. Induction of an α-helical structure upon interaction of membrane-active peptides with lipids is a common observation for such peptides [28,30,31]. Previous work [31,32], as well as our MC simulations and present findings with the charge variant, suggest that electrostatic interactions among the positively flanking regions of the SA segment and the anionic headgroups of the phospholipids probably contribute to this interaction. After the initial absorption, the SA segment reorganizes itself within the membrane and adopts a TM configuration. The driving force for this step is the free energy gain thanks to the hydrophobic effect, i.e. the non-polar interactions between the TM region and tails of phospholipid molecules surrounding it. Favourable electrostatic interactions between the flanking regions and the headgroups on both sides of the membrane further stabilize the TM configuration. The importance of the electrostatic interactions is reflected by a reduced calculated thermodynamic stability of a charge variant of OM45 and a reduced insertion of the corresponding protein or peptide into natural and artificial membranes. Furthermore, this working model is also in line with a previous study reporting that physiological membrane concentrations of anionic lipids greatly stabilize the TM configuration of a model hydrophobic segment with positively charged flanking regions [32].

A protein-free membrane-insertion mechanism was proposed to describe the integration of some tail-anchored proteins into the membranes of the ER and mitochondria [9,26,33]. It is also in line with previous studies that failed to identify a mitochondrial protein which is required for the membrane integration of OM45 and momMcr1 [12,13]. In contrast, Mim1 was reported to be required for the membrane insertion of Tom20 and Tom70, and/or for their assembly with the TOM complex [14–16]. However, the request for Mim1 and Tom40 in the biogenesis route of Tom receptors does not have to exclude a unified mechanism of initial insertion of SA proteins into the MOM. It might well be that all SA proteins follow initially a similar pathway of insertion that does not require additional proteins. According to this scenario, Mim1 is required for subsequent steps in the assembly of Tom20 and Tom70 with the rest of the TOM complex [15,34].

The apparently minor importance of proteins in assuring the specificity of the targeting and recognition processes raises the question of what other elements can mediate such distinct mitochondrial location. One such element can be the unique lipid composition of the MOM. Indeed, the SA peptide associated much better with lipid vesicles with the OM composition as compared with vesicles with ER-like composition. Thus we looked more closely at unique features of the lipid content of the MOM. For example, the MOM is the only one among all membranes facing the cytosol that contain the mitochondrial-specific phospholipid CL [19,35]. However, whereas this lipid seems to play a role in the association of apoptosis-regulating proteins with the OM [36,37], our results do not support a crucial role of CL in assuring specific membrane integration of OM45.

Low levels of ergosterol are another unique feature of the yeast MOM [38,39]. Indeed, our previous results with the tail-anchored protein Fis1 [9] and current findings with OM45 suggest that low ergosterol content is crucial for efficient membrane integration of OM single-span proteins. In addition to its well-known enhancement of the rigidity of the membrane, ergosterol might also influence the compressibility of the headgroups region. It has a relatively small headgroup allowing a more compact packing of the headgroup region of the bilayer [32,40]. Hence the elevated rigidity and reduced compressibility of sterol-containing membrane can result in compromised productive binding of signal-anchor peptides to this membrane.

In summary, we propose that newly synthesized mitochondrial SA protein might associate non-specifically and reversibly with various cellular membranes, but would bind productively, irreversibly and in a TM conformation only to the MOM. Although additional proteins can enhance the membrane integration process or preserve the SA protein in an insertion-competent conformation, we suggest that a distinct lipid composition of the MOM plays a primary role in the specific integration of SA proteins into this membrane.

AUTHOR CONTRIBUTION

Elisa Merklinger, Arnold Driessen, Nir Ben-Tal, Yechiel Shai and Doron Rapaport designed the research. Elisa Merklinger, Yana Gofman, Alexej Kedrov and Yechiel Shai performed the research. All authors analysed the data. Elisa Merklinger and Doron Rapaport wrote the paper.

ACKNOWLEDGEMENTS

We thank K. Rehn, E. Kracker and B. Zarmi for technical support, G. Schreiber and M. Harel for help with the stopped-flow setup, and K.S. Dimmer and M. Schuldiner for helpful discussions.

FUNDING

This work was supported by the Deutsche Forschungsgemeinschaft [grant number RA 1048/4–1 to D.R.] and a short-term fellowship from the Minerva Stiftung (to E.M.).

REFERENCES

1 Pfanner, N., Wiedemann, N., Meisinger, C. and Lithgow, T. (2004) Assembling the mitochondrial outer membrane. Nat. Struct. Mol. Biol. **11**, 1044–1048
2 Endo, T. and Yamano, K. (2009) Multiple pathways for mitochondrial protein traffic. Biol. Chem. **390**, 723–730
3 Walther, D. M. and Rapaport, D. (2009) Biogenesis of mitochondrial outer membrane proteins. Biochim. Biophys. Acta **1793**, 42–51
4 Shore, G. C., McBride, H. M., Millar, D. G., Steenaart, N. A. E. and Nguyen, M. (1995) Import and insertion of proteins into the mitochondrial outer membrane. Eur. J. Biochem. **227**, 9–18
5 Borgese, N., Colombo, S. and Pedrazzini, E. (2003) The tale of tail-anchored proteins: coming from the cytosol and looking for a membrane. J. Cell Biol. **161**, 1013–1019
6 Isenmann, S., Khew-Goodall, Y., Gamble, J., Vadas, M. and Wattenberg, B. W. (1998) A splice-isoform of vesicle-associated membrane protein-1 (VAMP-1) contains a mitochondrial targeting signal. Mol. Biol. Cell **9**, 1649–1660
7 Lan, L., Isenmann, S. and Wattenberg, B. W. (2000) Targeting and insertion of C-terminally anchored proteins to the mitochondrial outer membrane is specific and saturable but does not strictly require ATP or molecular chaperones. Biochem. J. **349**, 611–621
8 Horie, C., Suzuki, H., Sakaguchi, M. and Mihara, K. (2002) Characterization of signal that directs C-tail-anchored proteins to mammalian mitochondrial outer membrane. Mol. Biol. Cell **13**, 1615–1625

9 Kemper, C., Habib, S. J., Engl, G., Heckmeyer, P., Dimmer, K. S. and Rapaport, D. (2008) Integration of tail-anchored proteins into the mitochondrial outer membrane does not require any known import components. J. Cell Sci. **121**, 1990–1998

10 Schneider, H., Sollner, T., Dietmeier, K., Eckerskorn, C., Lottspeich, F., Trulzsch, B., Neupert, W. and Pfanner, N. (1991) Targeting of the master receptor MOM19 to mitochondria. Science **254**, 1659–1662

11 Schlossmann, J. and Neupert, W. (1995) Assembly of the preprotein receptor MOM72/MAS70 into the protein import complex of the outer membrane of mitochondria. J. Biol. Chem. **270**, 27116–27121

12 Ahting, U., Waizenegger, T., Neupert, W. and Rapaport, D. (2005) Signal-anchored proteins follow a unique insertion pathway into the outer membrane of mitochondria. J. Biol. Chem. **280**, 48–53

13 Meineke, B., Engl, G., Kemper, C., Vasiljev-Neumeyer, A., Paulitschke, H. and Rapaport, D. (2008) The outer membrane form of the mitochondrial protein Mcr1 follows a TOM-independent membrane insertion pathway. FEBS Lett. **582**, 855–860

14 Becker, T., Pfannschmidt, S., Guiard, B., Stojanovski, D., Milenkovic, D., Kutik, S., Pfanner, N., Meisinger, C. and Wiedemann, N. (2008) Biogenesis of the mitochondrial TOM complex: Mim1 promotes insertion and assembly of signal-anchored receptors. J. Biol. Chem. **283**, 120–127

15 Hulett, J. M., Lueder, F., Chan, N. C., Perry, A. J., Wolynec, P., Likic, V. A., Gooley, P. R. and Lithgow, T. (2008) The transmembrane segment of Tom20 is recognized by Mim1 for docking to the mitochondrial TOM complex. J. Mol. Biol. **376**, 694–704

16 Popov-Celeketic, J., Waizenegger, T. and Rapaport, D. (2008) Mim1 functions in an oligomeric form to facilitate the integration of Tom20 into the mitochondrial outer membrane. J. Mol. Biol. **376**, 671–680

17 Dukanovic, J. and Rapaport, D. (2011) Multiple pathways in the integration of proteins into the mitochondrial outer membrane. Biochim. Biophys. Acta **1808**, 971–980

18 Waizenegger, T., Stan, T., Neupert, W. and Rapaport, D. (2003) Signal-anchor domains of proteins of the outer membrane of mitochondria: structural and functional characteristics. J. Biol. Chem. **278**, 42064–42071

19 De Kroon, A. I. P. M., Koorengevel, M. C., Goerdayal, S. S., Mulders, P. C., Janssen, M. J. and De Kruijff, B. (1999) Isolation and characterization of highly purified mitochondrial outer membranes of the yeast *Saccharomyces cerevisiae*. Mol. Membr. Biol. **16**, 205–211

20 Ishiguro, R., Matsumoto, M. and Takahashi, S. (1996) Interaction of fusogenic synthetic peptide with phospholipid bilayers: orientation of the peptide alpha-helix and binding isotherm. Biochemistry **35**, 4976–4983

21 Sharon, M., Oren, Z., Shai, Y. and Anglister, J. (1999) 2D-NMR and ATR-FTIR study of the structure of a cell-selective diastereomer of melittin and its orientation in phospholipids. Biochemistry **38**, 15305–15316

22 Tamm, L. K. and Tatulian, S. A. (1997) Infrared spectroscopy of proteins and peptides in lipid bilayers. Q. Rev. Biophys. **30**, 365–429

23 Ghosh, J. K., Peisajovich, S. G. and Shai, Y. (2000) Sendai virus internal fusion peptide: structural and functional characterization and a plausible mode of viral entry inhibition. Biochemistry **39**, 11581–11592

24 Rosenfeld, Y., Barra, D., Simmaco, M., Shai, Y. and Mangoni, M. L. (2006) A synergism between temporins toward Gram-negative bacteria overcomes resistance imposed by the lipopolysaccharide protective layer. J. Biol. Chem. **281**, 28565–28574

25 Tang, J., Signarvic, R. S., DeGrado, W. F. and Gai, F. (2007) Role of helix nucleation in the kinetics of binding of mastoparan X to phospholipid bilayers. Biochemistry **46**, 13856–13863

26 Colombo, S. F., Longhi, R. and Borgese, N. (2009) The role of cytosolic proteins in the insertion of tail-anchored proteins into phospholipid bilayers. J. Cell Sci. **122**, 2383–2392

27 Huang, H. W. (2000) Action of antimicrobial peptides: two-state model. Biochemistry **39**, 8347–8352

28 White, S. H., Ladokhin, A. S., Jayasinghe, S. and Hristova, K. (2001) How membranes shape protein structure. J. Biol. Chem. **276**, 32395–32398

29 Shai, Y. (2002) Mode of action of membrane active antimicrobial peptides. Biopolymers **66**, 236–248

30 Andreev, O. A., Karabadzhak, A. G., Weerakkody, D., Andreev, G. O., Engelman, D. M. and Reshetnyak, Y. K. (2010) pH (low) insertion peptide (pHLIP) inserts across a lipid bilayer as a helix and exits by a different path. Proc. Natl. Acad. Sci. U.S.A. **107**, 4081–4086

31 van Klompenburg, W., Nilsson, I., von Heijne, G. and de Kruijff, B. (1997) Anionic phospholipids are determinants of membrane protein topology. EMBO J. **16**, 4261–4266

32 Shahidullah, K. and London, E. (2008) Effect of lipid composition on the topography of membrane-associated hydrophobic helices: stabilization of transmembrane topography by anionic lipids. J. Mol. Biol. **379**, 704–718

33 Brambillasca, S., Yabal, M., Makarow, M. and Borgese, N. (2006) Unassisted translocation of large polypeptide domains across phospholipid bilayers. J. Cell Biol. **175**, 767–777

34 Dimmer, S. K. and Rapaport, D. (2009) The enigmatic role of Mim1 in mitochondrial biogenesis. Eur. J. Cell Biol. **89**, 212–215

35 Gebert, N., Joshi, A. S., Kutik, S., Becker, T., McKenzie, M., Guan, X. L., Mooga, V. P., Stroud, D. A., Kulkarni, G., Wenk, M. R. et al. (2009) Mitochondrial cardiolipin involved in outer-membrane protein biogenesis: implications for Barth syndrome. Curr. Biol. **19**, 2133–2139

36 Kim, T. H., Zhao, Y., Ding, W. X., Shin, J. N., He, X., Seo, Y. W., Chen, J., Rabinowich, H., Amoscato, A. A. and Yin, X. M. (2004) Bid–cardiolipin interaction at mitochondrial contact site contributes to mitochondrial cristae reorganization and cytochrome C release. Mol. Biol. Cell **15**, 3061–3072

37 Gonzalvez, F., Schug, Z. T., Houtkooper, R. H., MacKenzie, E. D., Brooks, D. G., Wanders, R. J., Petit, P. X., Vaz, F. M. and Gottlieb, E. (2008) Cardiolipin provides an essential activating platform for caspase-8 on mitochondria. J. Cell Biol. **183**, 681–696

38 Zinser, E., Sperka-Gottlieb, C. D., Fasch, E. V., Kohlwein, S. D., Paltauf, F. and Daum, G. (1991) Phospholipid synthesis and lipid composition of subcellular membranes in the unicellular eukaryote *Saccharomyces cerevisiae*. J. Bacteriol. **173**, 2026–2034

39 Schneiter, R., Brugger, B., Sandhoff, R., Zellnig, G., Leber, A., Lampl, M., Athenstaedt, K., Hrastnik, C., Eder, S., Daum, G. et al. (1999) Electrospray ionization tandem mass spectrometry (ESI-MS/MS) analysis of the lipid molecular species composition of yeast subcellular membranes reveals acyl chain-based sorting/remodeling of distinct molecular species en route to the plasma membrane. J. Cell Biol. **146**, 741–754

40 Egashira, M., Gorbenko, G., Tanaka, M., Saito, H., Molotkovsky, J., Nakano, M. and Handa, T. (2002) Cholesterol modulates interaction between an amphipathic class A peptide, Ac-18A-NH2, and phosphatidylcholine bilayers. Biochemistry **41**, 4165–4172

Received 27 July 2011/22 November 2011; accepted 5 December 2011
Published as BJ Immediate Publication 5 December 2011, doi:10.1042/BJ20111363

Biochem. J. (2012) **442**, 381–389 (Printed in Great Britain) doi:10.1042/BJ20111363

online data

SUPPLEMENTARY ONLINE DATA

Membrane integration of a mitochondrial signal-anchored protein does not require additional proteinaceous factors

Elisa MERKLINGER*, Yana GOFMAN†, Alexej KEDROV‡, Arnold J. M. DRIESSEN‡, Nir BEN-TAL§, Yechiel SHAI¶ and Doron RAPAPORT*[1]

*Interfaculty Institute of Biochemistry, Hoppe-Seyler-Strasse 4, University of Tübingen, 72076 Tübingen, Germany, †Helmholtz-Zentrum, Max-Planck-Strasse 1, 21502 Geesthacht, Germany, ‡Department of Molecular Microbiology, Groningen Biomolecular Sciences and Biotechnology Institute and the Zernike Institute for Advanced Materials, University of Groningen, 9747 AG Groningen, The Netherlands, §Department of Biochemistry and Molecular Biology, The George S. Wise Faculty of Life Sciences, Tel Aviv University, Tel Aviv 69978, Israel, and ¶Department of Biological Chemistry, The Weizmann Institute of Science, Rehovot 76100, Israel

EXPERIMENTAL

Isolation of mitochondria by enzymatic spheroblastation

Preparation of crude mitochondria from cultures grown in lactate medium was performed as described previously [1]. Cells were harvested (3000 ***g***, 5 min, 20 °C), washed once in water, resuspended in 2 ml/g of cell weight of resuspension buffer [100 mM Tris base and 10 mM DTT (dithiothreitol), pH 9.4] and sedimented again. Cells were then washed with spheroblasting buffer (1.2 M sorbitol and 2 mM potassium phosphate buffer, pH 7.2) and cell walls were subsequently digested at 30 °C for 45 min in 6 ml/g of cell weight of the spheroblasting buffer supplemented with 1.1 mg/ml zymolyase (Seikagaku). All further steps were performed on ice or at 4 °C. Spheroblasts were collected by centrifugation (2000 ***g***, 5 min) resuspended in 100–200 ml of homogenization buffer (0.6 M sorbitol, 1 mM EDTA, 1 mM PMSF, 0.2 % fatty-acid-free BSA (Sigma), 10 mM Tris/HCl, pH 7.4) and lysed by ten strokes in a tight fitting Potter glass-glass homogenizer. Cell lysates were clarified by two centrifugation steps as described before and mitochondria were sedimented by centrifugation (18 000 ***g***, 12 min). Mitochondrial pellets were resuspended in 30 ml of SEM buffer (250 mM sucrose, 1 mM EDTA and 10 mM Mops-KOH, pH 7.2) containing 2 mM PMSF and clarified twice by centrifugation (2000 ***g***, 5 min). Mitochondria were re-isolated by centrifugation (18 000 ***g***, 12 min), resuspended in SEM buffer, aliquoted, snap-frozen in liquid nitrogen and stored at − 80 °C.

CD spectroscopy

The CD spectra of the peptide were recorded in an Aviv 202 spectropolarimeter in a thermostatically controlled quartz optical cell with a path length of 1 mm. Spectra were recorded at a wavelength range of 190–260 nm at 1 nm intervals with an average time of 6 s and three repetitions. The peptide was scanned at a concentration of 10 μM in two different environments: 5 mM Hepes buffer (pH 7.4), and the above buffer with 1 % LPC. The signals of the buffer and 1 % LPC before adding the peptide were subtracted from the signals after peptide addition.

Polarized ATR-FTIR analysis of the peptides

To determine the orientation of the peptide in lipid multibilayers, we used polarized ATR-FTIR spectroscopy. Spectra were recorded with a Bruker equinox 55 FTIR spectrometer equipped with a deuterated triacylglycerol sulfate detector coupled to an ATR device as described previously [2]. Briefly, prior to sample preparations, the TFA counter ions, which associate with the peptides, were replaced with chloride ions through several freeze-drying steps of the peptides in 0.1 M HCl. After the ion exchange, a mixture of phospholipid (1 mg) alone or with peptide (100 μg) was deposited on a germanium prism. The aperture angle of 45° yielded 25 internal reflections. Lipid/peptide mixtures were prepared by dissolving them together in a 1:2 $MeOH/CH_2Cl_2$ mixture and drying under vacuum for 15 min. Polarized spectra were recorded and the respective spectrum of pure phospholipid in each polarization was subtracted to yield the difference spectra in order to determine the amide I absorption peaks of the peptide. For each spectrum 60 scans were collected with a resolution of 4 cm^{-1}.

ATR-FTIR data analysis

Prior to curve fitting, a straight baseline passing through the ordinates at 1700 and 1600 cm^{-1} for the peptide, or 2800 and 3000 cm^{-1} for the lipids was subtracted. To resolve overlapping bands, we processed the spectra using PEAKFIT software (Jandel Scientific). Second-derivative spectra were calculated to identify the positions of the component bands. These wavenumbers were then used as initial parameters for curve fitting with Gaussian component peaks. Positions, band widths and amplitudes of the peaks were varied until (i) the resulting bands shifted by not more than 2 cm^{-1} from the initial parameters, (ii) all of the peaks had reasonable half-widths (<20–25 cm^{-1}) and (iii) there was good agreement between the calculated sum of all the components and the experimental spectra (r^2>0.99). The ATR electric fields of incident light were calculated as follows [3]:

$$E_x = \frac{2\cos\theta\sqrt{\sin^2\theta - n_{21}^2}}{\sqrt{(1-n_{21}^2)[(1+n_{21}^2)\sin^2\theta - n_{21}^2]}}$$

$$E_y = \frac{2\cos\theta}{(1-n_{21}^2)}$$

$$E_z = \frac{2\sin\theta\cos\theta}{\sqrt{(1-n_{21}^2)[(1+n_{21}^2)\sin^2\theta - n_{21}^2]}}$$

where θ is the angle of incidence between the light beam and the prism normal (45°) and n_{21} is the reflective index of the Ge

[1] To whom correspondence should be addressed (email doron.rapaport@uni-tuebingen.de).

(taken to be 4.03) divided by the reflective index of the membrane (taken to be 1.5). Under these conditions, E_x, E_y and E_z are 1.40, 1.52 and 1.64 respectively. The electric field components together with the dichroic ratio (defined as the ratio between absorption of parallel ($A_\parallel$) and perpendicular ($A_\perp$) polarized light, $R^{ATR} = A_\parallel / A_\perp$ are used to calculate the orientation order parameter, f, by the following formula:

$$R = \frac{A_\parallel}{A_\perp} = \frac{E_x^2}{E_y^2} + \frac{(E_z^2/E_y^2)(f\cos^2\alpha + (1-f)/3)}{(f\sin\alpha)/2 + (1-f)/3}$$

where α is the angle between the transition moment of the amide I vibration of the α-helix and the helix axis. We used the value of 27° for α as was previously suggested [3,4]. The orientation order parameter f allows calculating the 'average' angle of the peptide α-helices relative to the membrane normal by the following formula:

$$f = \frac{1}{2}[3(\cos^2\gamma)] - 1$$

Lipid order parameters were obtained from the lipid symmetric (2850 cm^{-1}) and asymmetric (2921 cm^{-1}) stretching mode using the same equations differing only by setting $\alpha = 90°$ [3].

Fluorescence measurements with a stopped-flow setup

The kinetics of peptide binding to LUVs was measured in a stopped-flow fluorimeter. The measurements were done at 25 °C with a slit width of 5 nm. The λ_{ex} was 467 nm and emission was detected using a cut-off filter of 520 nm. Every reaction was repeated at least six times, and the average signal was considered as the representative signal for the reaction. The association rate constants were measured in PBS under pseudo-first-order rate conditions. The data were fitted using a double exponent equation:

$$F(t) = \Delta F_1 \exp(^{-}k_{obs1}t) + \Delta F_2 \exp(^{-}k_{obs2}t) + F_\infty$$

where k_{obs1} and k_{obs2} are the observed rate constants for the first and second components of a double-exponential reaction and ΔF_1 and ΔF_2 are the amplitudes for the first and second components of a double-exponential reaction.

MC simulations

MC simulations of the OM45-SA peptide and its double mutant R4E, K26E were performed using the MCPep server (available online at http://bental.tau.ac.il/MCPep/). The membrane was represented as a smooth hydrophobic profile of native width of 30 Å (1 Å = 0.1 nm), corresponding to the hydrocarbon region. A negative surface charge was located on both sides of the membrane at a distance of 20 Å from the midplane. Its magnitude was estimated based on the relative fraction of charged lipids in the mitochondrial OM, i.e. 13 % (PI) + 2×4 % (CL) + 2 % (PS) = 23 %. The membrane was embedded in an aqueous solution of 0.1 M monovalent salt and pH 7.0, corresponding to physiological conditions. The initial peptide structure was constructed as a canonical α-helix and placed either in TM orientation with its principle axis roughly along the membrane normal or surface orientation with its axis roughly in the membrane surface. The MCPep server calculated the free energy of each configuration in comparison with the free energy in the aqueous phase.

Received 27 July 2011/22 November 2011; accepted 5 December 2011
Published as BJ Immediate Publication 5 December 2011, doi:10.1042/BJ20111363

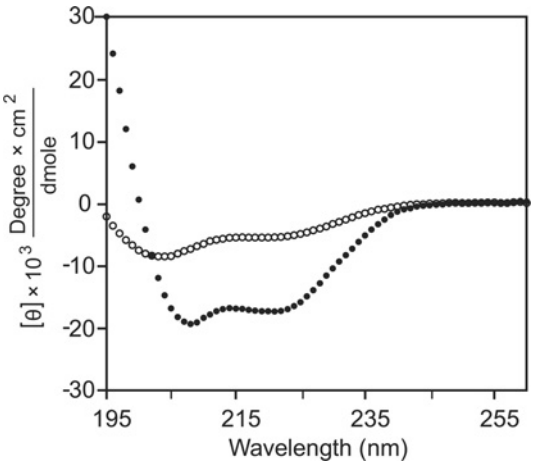

Figure S1 CD spectra of the OM45-SA peptide

Freeze-dried samples of peptide were dissolved directly in buffer (pH 7.4) (open circles) or in buffer containing 1 % (w/v) LPC (closed circles). The spectra were taken at peptide concentrations of 10 μM.

Table S1 Peptide secondary structure in buffer (pH 7.4) and in buffer + 1 % LPC determined by CD spectroscopy

	Secondary structure (%)	
	Buffer	Buffer + 1 % LPC
α-Helix	17	58
β-Sheet	32	9
Random coil	33	18
Other	18	15

REFERENCES

1 Daum, G., Gasser, S. and Schatz, G. (1982) Import of proteins into mitochondria: energy-dependent, two-step processing of the intermembrane space enzyme cytochrome b_2 by isolated yeast mitochondria. J. Biol. Chem. **257**, 13075–13080
2 Gazit, E., Miller, I. R., Biggin, P. C., Sansom, M. S. and Shai, Y. (1996) Structure and orientation of the mammalian antibacterial peptide cecropin P1 within phospholipid membranes. J. Mol. Biol. **258**, 860–870
3 Ishiguro, R., Matsumoto, M. and Takahashi, S. (1996) Interaction of fusogenic synthetic peptide with phospholipid bilayers: orientation of the peptide alpha-helix and binding isotherm. Biochemistry **35**, 4976–4983
4 Rothschild, K. J. and Clark, N. A. (1979) Polarized infrared spectroscopy of oriented purple membrane. Biophys. J. **25**, 473–487